

Stress measurements of planar dielectric elastomer actuators

Bekim Osmani, Elise A. Aeby, and Bert Müller

Citation: *Review of Scientific Instruments* **87**, 053901 (2016); doi: 10.1063/1.4949519

View online: <http://dx.doi.org/10.1063/1.4949519>

View Table of Contents: <http://scitation.aip.org/content/aip/journal/rsi/87/5?ver=pdfcov>

Published by the [AIP Publishing](#)

Articles you may be interested in

[Inhibiting electro-thermal breakdown of acrylic dielectric elastomer actuators by dielectric gel coating](#)
Appl. Phys. Lett. **108**, 012903 (2016); 10.1063/1.4939550

[Saddle-like deformation in a dielectric elastomer actuator embedded with liquid-phase gallium-indium electrodes](#)
J. Appl. Phys. **116**, 144905 (2014); 10.1063/1.4897551

[Giant voltage-induced deformation of a dielectric elastomer under a constant pressure](#)
Appl. Phys. Lett. **105**, 112901 (2014); 10.1063/1.4895815

[Computational model of deformable lenses actuated by dielectric elastomers](#)
J. Appl. Phys. **114**, 104104 (2013); 10.1063/1.4821028

[Thickness dependence of curvature, strain, and response time in ionic electroactive polymer actuators fabricated via layer-by-layer assembly](#)
J. Appl. Phys. **109**, 104301 (2011); 10.1063/1.3590166



Stress measurements of planar dielectric elastomer actuators

Bekim Osmani, Elise A. Aeby, and Bert Müller

Biomaterials Science Center, University of Basel, Gewerbestrasse 14, 4123 Allschwil, Switzerland

(Received 6 December 2015; accepted 2 May 2016; published online 17 May 2016)

Dielectric elastomer actuator (DEA) micro- and nano-structures are referred to artificial muscles because of their specific continuous power and adequate time response. The bending measurement of an asymmetric, planar DEA is described. The asymmetric cantilevers consist of 1 or 5 μm -thin DEAs deposited on polyethylene naphthalate (PEN) substrates 16, 25, 38, or 50 μm thick. The application of a voltage to the DEA electrodes generates an electrostatic pressure in the sandwiched silicone elastomer layer, which causes the underlying PEN substrate to bend. Optical beam deflection enables the detection of the bending angle vs. applied voltage. Bending radii as large as 850 m were reproducibly detected. DEA tests with electric fields of up to 80 V/ μm showed limitations in electrode's conductivity and structure failures. The actuation measurement is essential for the quantitative characterization of nanometer-thin, low-voltage, single- and multi-layer DEAs, as foreseen for artificial sphincters to efficiently treat severe urinary and fecal incontinence. *Published by AIP Publishing.* [<http://dx.doi.org/10.1063/1.4949519>]

I. INTRODUCTION

Dielectric elastomer actuators (DEAs) consist of electrically insulating membranes sandwiched between compliant electrodes. Their performance characteristics, i.e., lateral strains similar to mammalian skeletal muscles¹ and millisecond response times,² offer a wide variety of applications including artificial muscles.³ Using polydimethylsiloxane (PDMS) as an elastomer membrane, electrical fields of 100 V/ μm are required to generate strains comparable to human skeletal muscles.⁴ Current research activities for medical applications⁵ focus on the reduction of the operation voltage to a few 10 V, which implies the fabrication of sub-micrometer-thin elastomer layers. In order to reach the necessary actuation forces⁶ multilayer devices have to be built. A proper characterization of the accessible strain levels as the function of the applied voltage is, therefore, crucial to improving future DEA devices. Recently, the critical need for standardization of dielectric elastomer transducers has been addressed.⁷ The present communication presents a compact cantilever-based setup to reproducibly and precisely measure the actuation forces and the related strains of DEAs. DEAs are especially interesting since they can also operate in sensor mode.⁸

Cantilever bending is well known, e.g., from atomic force microscopy and heteroepitaxy studies.⁹ In static mode, they can act as mechanical sensors to measure surface stress.^{10–12} Force sensing via cantilevers was also shown for a zinc oxide film sandwiched between two electrodes.¹³ Disposable polymer micromechanical cantilever arrays were fabricated by means of vario-thermal micro-injection molding techniques¹⁴ and were used to detect single-stranded DNA sequences and metal ions. In cell biology and for the characterization of biomaterials cantilevers serve for the determination of contractile cell forces. For example, an ensemble of fibroblasts seeded to a single-crystalline silicon cantilever can be detached by means of trypsin and the related cantilever relaxation

monitored.¹⁵ Elastic and shear moduli were measured using cantilevers with a piezoelectric layer on a stainless steel plate. The electric field causes the cantilever to bend compressing the softer substrate.¹⁶ Bending is usually detected using (i) piezoresistive or piezoelectric readout techniques or (ii) optical methods including the interferometry-based and the beam-deflection readout, which is most common because of simplicity and lateral resolution.¹⁷

II. EXPERIMENT

A. Fabrication of DEA on polyethylene naphthalate (PEN) cantilever

Biaxially oriented polyethylene naphthalate (PEN) sheets (Teonex[®] Q51, Synflex, Germany) 16, 25, 38, or 50 μm thick in A4-format were weighted with an electronic laboratory balance (Shimadzu Corporation, Type UW620HV, readability of 0.001 g) to verify their average thicknesses, cf., Table I. The PEN sheets were cut to the size of 3 in. wafers and cleaned by ethanol. In order to keep the substrates planar, we have deployed single-crystalline 3 in. Si wafers as a mechanical support.

The backside of the PEN substrate was coated with a 20 nm thin Au film using a DC magnetron sputter coater (SCD040, Balzers Union, Liechtenstein) at a discharge current of 15 mA in a 0.05 mbar Ar-atmosphere and served as a reflective layer. A quartz crystal microbalance (QSG 301, Balzers Union, Liechtenstein) monitored the deposition.

On the front size of the PEN substrate, the DEA films were fabricated. The 20 nm-thin Au electrodes were sputtered through Mo masks under the same conditions as the reflective layer. The seven windows in the Mo masks, each 4 mm \times 22 mm, were cut using a pulsed Nd:YAG solid-state laser. Subsequent to the sputtering of the first Au electrodes the elastomer layers were spin-coated (WS-400B-6NPP/LITE/AS, Laurell Technologies Corporation, North

TABLE I. Geometrical parameters of the PEN cantilevers with DEA on top.

Sample	PEN cantilever			DEA layer thickness		
	Thickness (μm)	Width (mm)	Length (mm)	Elastomer (μm)	Electrodes (nm)	Reflective layer (nm)
#1	16 ± 0.3	4 ± 0.5	12 ± 1	1.0 ± 0.2	20 ± 2	20 ± 2
#2	25 ± 0.5	4 ± 0.5	12 ± 1	1.3 ± 0.3	20 ± 2	20 ± 2
#3	38 ± 0.6	4 ± 0.5	12 ± 1	5.0 ± 1	20 ± 2	20 ± 2
#4	50 ± 0.8	4 ± 0.5	12 ± 1	5.0 ± 1	20 ± 2	20 ± 2

Wales, PA, USA) with a rotation speed of 6000 rpm for the duration of 2 min. For this purpose, the two liquid components of the silicone elastomer kit, Dow Corning® 184 Silicone Elastomer Kit, Dow Corning Europe S.A, Belgium, were mixed and degassed for a 30 min period. For the preparation of the films marked #1 and #2, the methylsiloxane-based solvent, Dow Corning® OS-20 Fluid, Dow Corning Europe S.A, Belgium, was added to 10 ml containers at a ratio of 1:5 to reduce the obtained film thickness. Seven PEN cantilevers with the DEA on top, see scheme in Figure 1(a), were cut off with a standard roller cutter from each 3 in. PEN substrate.

The 3D Laser Microscope Keyence VK-X200, Keyence International, Belgium, was used to measure the film thickness with a spatial resolution of 0.5 nm. Table I lists the results of the thickness measurements.

In order to contact the bottom Au electrode, a 3 mm broad stripe of the PDMS-layer was removed through washing in ethyl acetate immediately after spin coating. In a next step, the PDMS was thermally cured at a temperature of 75 °C for a period of 24 h. Finally, the film for the other electrodes was sputtered on the cured PDMS layer.

DEA/PEN cantilevers 22 mm long and 4 mm wide were cut out of the processed PEN substrate and mounted on a polytetrafluoroethylene (PTFE) holder so that the free-standing area of 12 mm \times 4 mm could contribute to the actuation. Figure 1 displays (a) the DEA design on the PEN cantilever, (b) the mounting on the PTFE holder with the organization of the electrical contacts, and (c) the scheme of the bending mechanism for the anisotropic microstructure.

The DEA was powered with either the source Stanford Research System PS310, GMP SA, Lausanne, Switzerland or the Amplifier Nanobox USB, Piezosystem Jena GmbH, Germany. The applied voltage was monitored using the portable high-voltage USB oscilloscope Handyprobe HP3-5, TiePie Engineering, Holland.

The mechanical properties of the DEA structure were assessed by the atomic force microscope FlexAFM C3000, Nanosurf AG, Switzerland. To this end, 400 indentation measurements on 60 μm \times 60 μm arrays at a load of 100 nN using a spherical tip with a radius of 500 nm (B500_FMR, Nanotools GmbH, Germany) were acquired. The mean Young's modulus of DEA microstructures was calculated using the FLEX-ANA® (Automated Nanomechanical Analysis) software from Nanosurf. Potential effects of the PEN substrate were neglected since the indentation depths were well below 500 nm.

B. Bending radius measurements of the DEA/PEN cantilever

The apparatus consists of two compartments, labeled (A) and (B), as shown in Figure 2(a). In the temperature-controlled chamber with the label (A), the DEA/PEN cantilever is mounted on a PTFE holder and connected to the power source. This compartment has three DN 50 mm openings that allow for the visual inspection and keeping records with a camera. The opening on the back gives direct access

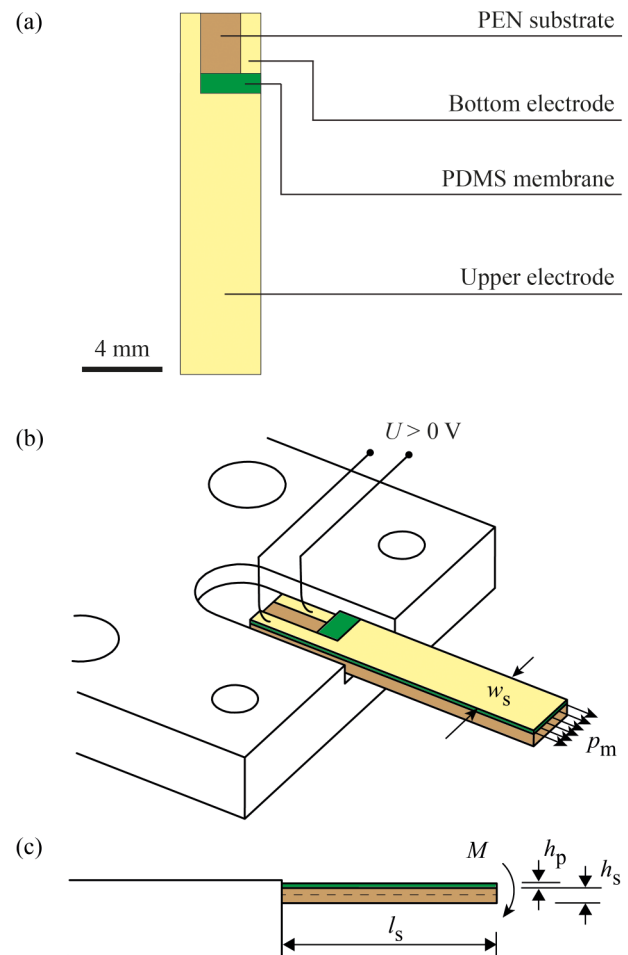


FIG. 1. Completion of the DEA/PEN cantilever. (a) Top view of the cantilever showing the sandwiched PDMS layer on the PEN substrate. (b) DEA/PEN cantilever mounted on a grooved PTFE holder and with an illustration of the electrical contacts. The Maxwell pressure p_m in the elastomer film induces the torque M . (c) Side view of the cantilever including the main geometrical parameters.

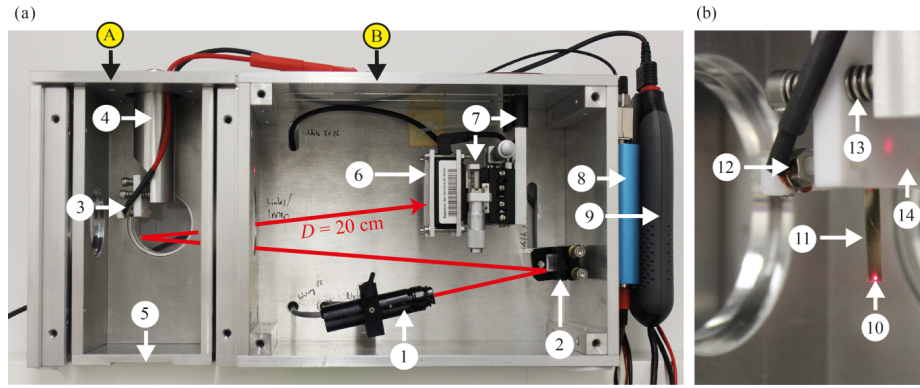


FIG. 2. Apparatus for bending measurements of the DEA/PEN cantilever. The voltage-induced bending of the DEA cantilever is detected by the optical beam-deflection method. The vertical arrangement of the cantilever prevents a gravity-induced bending. The rotation of the apparatus around its axis can be used for calibration purposes as described below. (a) The photograph shows the compartment for the cantilever, labeled (A) and the one for the optical detection, labeled (B). The path of the laser beam is drawn in red color. (b) The detailed view displays the positioning of the cantilever. The main components of the apparatus are (1) the diode laser L2S-WEB-SL, Laser 2000 GmbH, Germany, (2) the broadband mirror, Thorlabs GmbH, Germany, (3) the cantilever holder made from PTFE, (4) the rotatable support for the cantilever holder, (5) two Peltier elements 6.3 A/65 W/16.7 V/74 K, Deltron AG, Switzerland, (6) the PSD SPOTCOM-L09, Duma Optronics Ltd., Israel, (7) the two-dimensional linear translation stage, Newport, Taiwan, (8) the amplifier Nanobox USB, Piezosystem Jena GmbH, Germany, (9) the oscilloscope Handyprobe HP3-5, TiePie Engineering, Holland, (10) the reflected laser beam on the backside of the Au-coated cantilever, (11) the DEA/PEN cantilever, (12) the support for the electrical contacts, (13) the screws for adjusting the beam direction, and (14) the PTFE cantilever holder.

to the cantilever. The PTFE cantilever holder is mounted on a rotatable solid aluminum arm with three screw/spring joints to adjust the direction of the reflected laser beam, as shown in Figure 2(b). Note that the actuators will be integrated into medical implants intended to operate at body temperature, and the DEA is sensitive to ambient air conditions. Flooding the compartment with rare gases or nitrogen at well-defined temperature is therefore a key feature of the apparatus.

The compartment (B) contains the elements for the optical detection of the cantilever bending, i.e., the laser, a mirror, and the position-sensitive detector (PSD). The size of the PSD is 9 mm × 9 mm and has a position accuracy of ±12.5 μm. It can be translated in two directions by means of a linear translation stage and in the third direction using rails on top of the apparatus.

An input of electrical energy by applying a voltage U to the DEA with the related electrostatic pressure p_m acting on the elastomer film leads to a torque that bends the asymmetric cantilever. The laser beam is reflected on the back side of the Au-coated cantilever and is positioned close to its free end. The sensitivity of the system depends on the cantilever length l_s and the distance D between cantilever and PSD. The choice of these two parameters allows measuring of actuation forces as small as 0.1 N. The curvature of the cantilever k_s , i.e., the inverse bending, is derived from the displacement d of the laser beam on the PSD,

$$k_s = \frac{1}{2Dl_s}d = 208 \frac{1}{\text{m}^2}d. \quad (1)$$

The displacement d is directly provided by the optical beam position and power measurement system (SpotON, Version 5.30.1, Duma Optronics Ltd., Israel) that controls the 24 bit A/D electronics box via the USB 2.0 port at an update rate of 50 Hz.

III. RESULTS AND DISCUSSION

A. Calibration

Equation (2) describes the gravity-driven deflection of the neutral axis $\delta(x)$ for a one-sided fixed horizontal cantilever determined by its free length l_s , the elastic modulus E_s , and the area moment of inertia I_s ,¹⁸

$$\delta(x) = \frac{q}{24E_sI_s}(x^4 - 4l_sx^3 + 6l_s^2x^2). \quad (2)$$

The deflection at the apex δ_t for $x = l_s$ yields to

$$\delta_t = \delta_{x=l_s} = \frac{ql_s^4}{8E_sI_s}. \quad (3)$$

The curvature k_s can be approximated using the deflection at apex and cantilever length,¹⁰

$$k_s \approx \frac{2\delta_t}{l_s^2}. \quad (4)$$

Thus, assuming the uniform load $q = mg/l_s$, the curvature k_s depends on the cantilever orientation φ ,

$$k_s = \frac{mgl_s}{4E_sI_s} \sin \varphi, \quad (5)$$

where m is the total mass, here the one of the PEN substrate including the DEA structure. Because of the area momentum of inertia I_s , the value of the average cantilever thickness h_s has to be precisely known. The data of the manufacturer should be verified. Here, the rotation of the apparatus, which is displayed in Figure 2(a), around the perpendicular axis is useful. One can easily measure the curvature k_s , for example, in angular steps of 30° along 720°. Figure 3(a) shows such experimental data with the plotted Equation (5) for the substrate only and for the substrate with a fabricated DEA on top. The error indicates reasonable reliability and reproducibility. Using Equation (5), the curvature is converted into the thickness

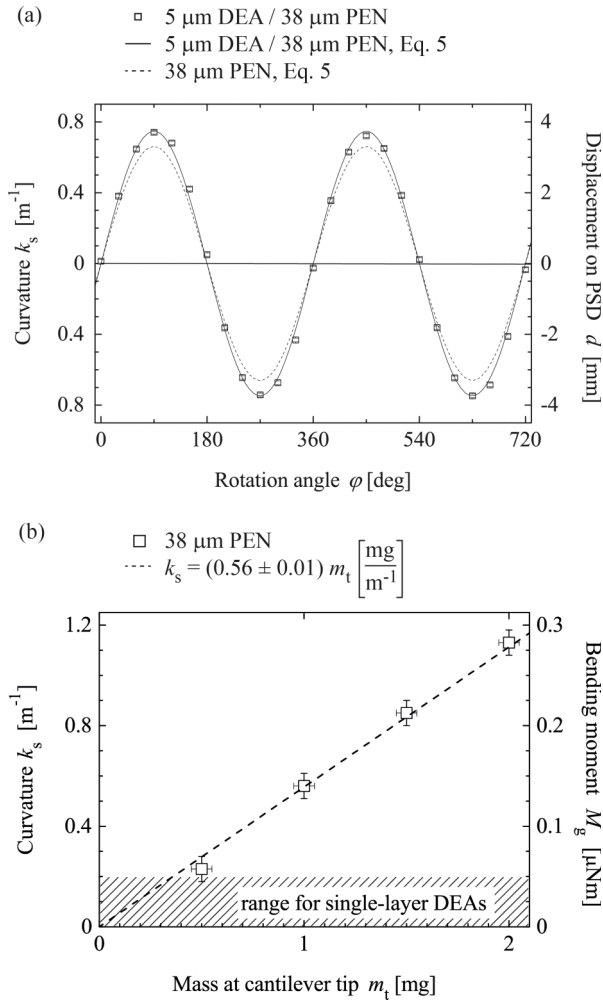


FIG. 3. Calibration of the PEN cantilever. (a) The system is calibrated, rotating the apparatus around its perpendicular axis and measuring the gravity-induced displacement on the PSD for the selected angles. The amplitude of the fitted sine is compared with the prediction for a one-sided fixed horizontal beam under a uniformly distributed load. (b) The curvature k_s was measured for selected amounts of water placed near the tip of the cantilever in Al container. The system shows a linear behavior for bending radii larger than 1 m.

$h_s = (37.7 \pm 0.6) \mu\text{m}$, a value that corresponds to the information of the manufacturer.

To verify the linear behavior of the cantilever deflection in the stress interval of interest, an increasing amount of water was put in an Al container near the free end of the horizontally oriented cantilever. To this end, a single-channel micropipette with 2 μl water (Finnpipette, Labsystems 4500, Finland) was applied. Figure 3(b) summarizes a selected series of experiments, which demonstrate the linearity for curvatures of up to 1 m⁻¹. Therefore, the method allows testing multi-layer DEAs, if a single-layer DEA produces curvatures of up to 0.2 m⁻¹ as for the present experiment.

An alternative to determine the geometrical and mechanical parameters of the cantilever is the measurement of the flexural bending frequencies. Utilizing the presented experimental setup, however, a reliable analysis was only possible with single-crystalline Si cantilevers and not with the much softer PEN.

B. Background

The dependence between the curvature k_s of the cantilever and the voltage U applied to the DEA microstructure on top should be predicted. The DEA with an elastomer thickness h_p and a relative permittivity ϵ can transduce the applied voltage U into mechanical work according to the Maxwell stress,¹⁹ generally termed as the actuation pressure p_m ,

$$p_m = \epsilon_0 \epsilon \frac{U^2}{h_p^2}. \quad (6)$$

The generated force F for a single-layer DEA is length independent. It is determined by the cross-sectional area A , given by the width w and height h_p ,

$$F = p_m A = p_m h_p w = \epsilon_0 \epsilon \frac{U^2}{h_p} w. \quad (7)$$

Since the Young's modulus of the substrate is about three orders of magnitude higher than the one of the deposited DEA, the induced bending moment M on the asymmetric cantilever with the thickness h_s can be written as

$$M = F \left(\frac{h_s}{2} + \frac{h_p}{2} \right). \quad (8)$$

Using the differential equation for the deflection of an elastic beam,¹⁰ the curvature k_s for small deflections is known as

$$k_s = \frac{1}{R} \cong \frac{\partial^2 z}{\partial x^2} \cong \frac{M}{E^* I} = \frac{M(1 - \nu_s)}{E_s I_s}, \quad (9)$$

with E^* as the biaxial modulus²⁰ that relates to the Young's modulus E_s and the Poisson's ratio ν_s as $E^* = E_s / (1 - \nu_s)$. Replacing the area moment of inertia of the cantilever using $I_s = (wh_s^3)/12$, the curvature k_s can be expressed as a function

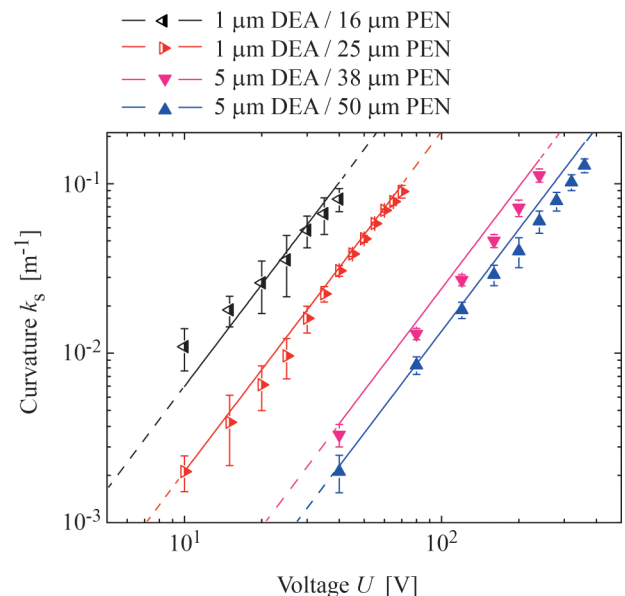


FIG. 4. Actuation of DEA on PEN-cantilevers as a function of the applied voltage U . The error bars correspond to the standard deviation obtained from multiple measurements. The lines originate from the predictions according to Equation (10).

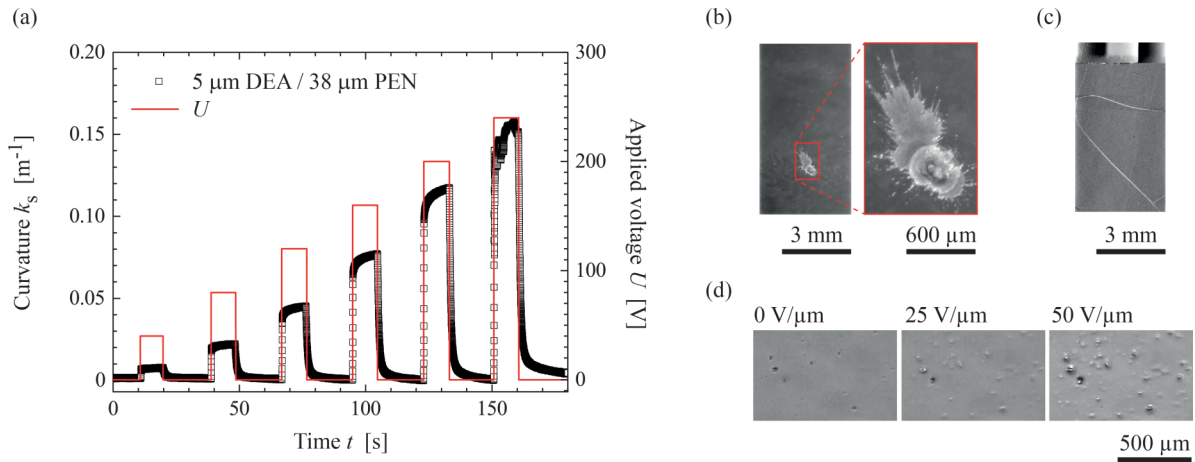


FIG. 5. (a) The curvature measurements with a 50 Hz sampling rate demonstrate the time response of the DEA/PEN actuator to voltages applied for a duration of 10 s. The application of 240 V resulted in a discontinuous behavior, which indicates the formation of changes within the Au electrodes. (b) The optical micrograph of the DEA electrode acquired with two magnifications shows the morphology after dielectric breakdown. (c) Optical micrograph to demonstrate the formation of characteristic cracks. (d) The series of optical micrographs indicates morphological changes as the function of the applied electric field. The values are given above each image.

of U^2 and a constant term

$$k_s = \frac{F(h_p + h_s)(1 - \nu_s)}{2E_s I_s} = U^2 \frac{6\varepsilon_o \varepsilon (h_p + h_s)(1 - \nu_s)}{E_s h_p h_s^3}. \quad (10)$$

C. Actuation curves for single-layer DEA on PEN cantilever

Figure 4 shows the actuation behavior of DEA/PEN cantilevers applying voltages U between 10 and 370 V. The 5 μm -thick elastomer films were deposited on the 38 and 50 μm -thick PEN-substrates. As the DEA structures with a thickness of 1 μm evolve smaller bending moments than the 5 μm -thick microstructures, they were prepared on 16 and 25 μm -thin PEN-substrates. For these thinner DEA-microstructures, the voltage was limited to 72 V to prevent the electrical breakdown. The precise value depends on humidity, temperature, film thickness, elastomer pre-stretching, and the stiffness of the electrodes.^{7,21,22} The maximal curvatures were below 0.1 m^{-1} . Therefore, the experiments only cover the linear regime. Figure 4 represents the obtained actuation data on a double-logarithmic plot and demonstrates the quadratic dependence of the curvature k_s from the applied voltage U . The system allows detecting bending radii R up to 850 m, which corresponds to $k_s = 0.0012 \text{ m}^{-1}$. The experimental data reasonably agree with the ones predicted from Equation (10), cf., Figure 4.

D. Real-time measurement of actuation curves

Figure 5(a) displays experimental data on the temporal response of a DEA/PEN cantilever to rectangular voltage pulses with a duration of 10 s. The actuator reacts with the expected millisecond response.² Especially for the higher voltages, however, one clearly observes a creep. This creep may originate from the viscoelastic deformation of the PDMS membrane and the morphology changes of the relatively stiff electrodes with forming cracks owing to the areal strain.^{23–25} The integration of an adhesive layer can prevent the crack

formation and allows for significantly larger electric fields.²⁶ The areal strain in the top electrode depends on the Young's modulus of the DEA and the applied voltage U . Assuming a uniform electric field at a voltage of 240 V and a Young's modulus of (411 ± 38) kPa, as experimentally derived, the areal strain of a free standing membrane corresponds to 6.7%. As the DEA/PEN cantilevers are one-side constrained, the electro-creasing to cratering instability has to be considered. This phenomenon can be suppressed or delayed by stiffening or pre-stretching the elastomers. The electrical energy density u_{max} is a critical performance parameter for DEA and expressed as²⁷

$$u_{\text{max}} = Z\mu = \varepsilon \frac{E_b^2}{2}. \quad (11)$$

Assuming the parameters $Z = 0.53$, $\varepsilon = 2.7\varepsilon_0$, and $\mu = 137$ kPa for the PDMS used, the derived value for the breakdown voltage $E_b = 78 \text{ V}/\mu\text{m}$ corresponds well to the experimental results of the present study. Gatti *et al.* have shown recently that the dielectric breakdown limit depends on its thickness and the pre-stretch ratio.²⁸ They have identified a value of about 70 $\text{V}/\mu\text{m}$ for a 20 μm -thin PDMS membrane. Figure 5(b) shows selected optical micrographs of a DEA/PEN cantilever after electrical breakdown.

As displayed in Figure 5(a), the discontinuous curvature changes during the application of a constant voltage as high as 240 V implying local structural failures and the significant formation of cracks, as shown in Figure 5(c). Structural changes can even be recognized well below the breakdown voltage, cf., the series of optical micrographs in Figure 5(d). The magnitudes of the applied electrical fields are displayed above the micrographs.

IV. CONCLUSIONS

A compact, portable apparatus to measure the actuation of DEA on micrometer-thin polymer cantilevers was designed, built, and brought into operation. The detected actuation values

correspond reasonably well to the predictions. The actuation force F of a single-layer DEA calculated from Equation (10) is below 1 mN. The apparatus is therefore well suited also for the characterization of multi-layer actuators. The electrical breakdown is observed at 80 V/ μm that is smaller than the dielectric strength of 140 V/ μm reported for the used silicon elastomer⁸ (Dow Corning[®] Sylgard 184). We presume that impurities and thickness variations within the elastomer layer caused the reduction. The presented apparatus for measuring the voltage-dependent curvature will allow improving the actuator performance that includes the long-term behavior.

ACKNOWLEDGMENTS

The financial support of the nano-tera.ch initiative, project SmartSphincter, is gratefully acknowledged. The authors thank Sascha Martin from the machine shop at the Physics Department of the University Basel for the manufacturing of the mechanical components. Synflex GmbH, Germany kindly provided the PEN Teonex[®] Q51 substrates. The authors also thank Monica Schönenberger from the Nanotech Service Lab for her assistance at the 3D Laser microscope as well as Tino Töpfer, Vanessa Leung, and Florian Weiss for their support in component selection and discussion of technical details.

- ¹J. D. W. Madden, N. A. Vandesteeg, P. A. Anquetil, P. G. A. Madden, A. Takshi, R. Z. Pytel, S. R. Lafontaine, P. A. Wieringa, and I. W. Hunter, *IEEE J. Oceanic Eng.* **29**(3), 706–728 (2004).
- ²R. Pelrine, *Science* **287**(5454), 836–839 (2000).
- ³Y. Bar-Cohen, *Electroactive Polymer (EAP) Actuators as Artificial Muscles: Reality, Potential, and Challenges* (SPIE Press, 2004).
- ⁴B. Müller, H. Deyhle, S. Mushkolaj, and M. Wieland, *Swiss Med. Wkly* **139**(41-42), 591–595 (2009).
- ⁵T. Töpfer, F. M. Weiss, B. Osmani, C. Bippes, V. Leung, and B. Müller, *Sens. Actuators, A* **233**, 32–41 (2015).
- ⁶A. O'Halloran, F. O'Malley, and P. McHugh, *J. Appl. Phys.* **104**(7), 071101 (2008).
- ⁷F. Carpi, I. Anderson, S. Bauer, G. Frediani, G. Gallone, M. Gei, C. Graaf, C. Jean-Mistral, W. Kaal, and G. Kofod, *Smart Mater. Struct.* **24**(10), 105025 (2015).
- ⁸P. Brochu and Q. Pei, *Macromol. Rapid Commun.* **31**(1), 10–36 (2010).
- ⁹D. Sander, A. Enders, and J. Kirschner, *Rev. Sci. Instrum.* **66**(9), 4734–4735 (1995).
- ¹⁰M. Godin, V. Tabard-Cossa, P. Grütter, and P. Williams, *Appl. Phys. Lett.* **79**(4), 551–553 (2001).
- ¹¹C. A. Klein, *J. Appl. Phys.* **88**(9), 5487–5489 (2000).
- ¹²M. Liangruksa, Master thesis, Virginia Polytechnic Institute and State University, Virginia, 2008.
- ¹³T. Itoh and T. Suga, *Appl. Phys. Lett.* **64**(1), 37–39 (1994).
- ¹⁴P. Urwyler, O. Häfeli, H. Schiff, J. Gobrecht, F. Battiston, and B. Müller, *Procedia Eng.* **5**, 347–350 (2010).
- ¹⁵J. Köser, S. Gaiser, and B. Müller, *Eur. Cells Mater.* **21**, 479–487 (2011), <http://www.ncbi.nlm.nih.gov/pubmed/21623572>.
- ¹⁶A. Markidou, W. Y. Shih, and W. H. Shih, *Rev. Sci. Instrum.* **76**(6), 064302 (2005).
- ¹⁷M. Bicker, U. Von Hülsen, U. Laudahn, A. Pundt, and U. Geyer, *Rev. Sci. Instrum.* **69**, 460–462 (1998).
- ¹⁸W. Flügge, *Handbook of Engineering Mechanics* (McGraw-Hill, New York, 1962).
- ¹⁹R. Pelrine, R. Kornbluh, J. Joseph, R. Heydt, Q. Pei, and S. Chiba, *Mater. Sci. Eng. C* **11**(2), 89–100 (2000).
- ²⁰T. Miyatani and M. Fujihira, *J. Appl. Phys.* **81**(11), 7099–7115 (1997).
- ²¹B. Osmani, T. Töpfer, C. Deschenaux, J. Nohava, F. M. Weiss, V. Leung, and B. Müller, *AIP Conf. Proc.* **1646**(1), 91–100 (2015).
- ²²S. Rosset and H. Shea, *Appl. Phys. A* **110**(2), 281–307 (2013).
- ²³I. M. Graz, D. P. Cotton, and S. P. Lacour, *Appl. Phys. Lett.* **94**(7), 071902 (2009).
- ²⁴T. Töpfer, B. Osmani, F. M. Weiss, C. Winterhalter, F. Wohlfender, V. Leung, and B. Müller, *Proc. SPIE* **9430**, 94300B (2015).
- ²⁵K. Jia, T. Lu, and T. J. Wang, *Sens. Actuators, A* **239**, 8–17 (2016).
- ²⁶B. Osmani, H. Deyhle, F. M. Weiss, T. Töpfer, M. Karapetkova, V. Leung, and B. Müller, *Proc. SPIE* **9798**, 979822 (2016).
- ²⁷X. Zhao and Q. Wang, *Appl. Phys. Rev.* **1**(2), 021304 (2014).
- ²⁸D. Gatti, H. Haus, M. Matysek, B. Frohnapfel, C. Tropea, and H. F. Schlaak, *Appl. Phys. Lett.* **104**(5), 052905 (2014).